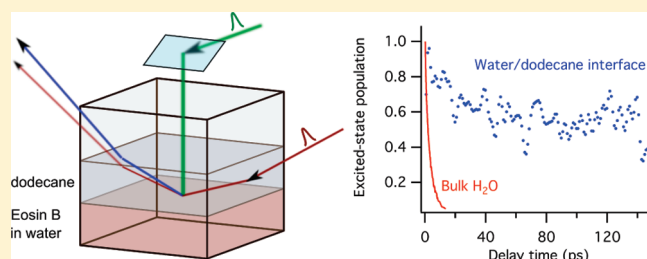# Hydrogen-Bond-Assisted Excited-State Deactivation at Liquid/Water Interfaces

Piotr Fita,[†] Marina Fedoseeva, and Eric Vauthey*

Department of Physical Chemistry, University of Geneva, 30 Quai Ernest-Ansermet, CH-1211 Geneva 4, Switzerland

ABSTRACT: The excited-state dynamics of eosin B (EB) at dodecane/water and decanol/water interfaces has been investigated with polarization-dependent and time-resolved surface second harmonic generation. The results of the polarization-dependent measurements vary substantially with (1) the EB concentration, (2) the age of the sample, and (3) the nature of the organic phase. All of these effects are ascribed to the formation of EB aggregates at the interface. Aggregation also manifests itself in the time-resolved measurements as a substantial shortening of the excited-state lifetime of EB. However, independently of the dye concentration used, the excited-state lifetime of EB at both dodecane/water and decanol/water interfaces is much longer than in bulk water, where the excited-state population undergoes hydrogen-bond-assisted non-radiative deactivation in a few picoseconds. These results indicate that hydrogen bonding between EB and water molecules at liquid/water interfaces is either much less efficient than in bulk water or does not enhance non-radiative deactivation. This strong increase of the excited-state lifetime of EB at liquid/water interfaces opens promising avenues of applying this molecule as a fluorescent interfacial probe.

INTRODUCTION

Over the past few years, second-order nonlinear optical techniques, such as surface second harmonic generation (SSHG)[1−3] and surface sum frequency generation (SSFG),[4,5] have become powerful and extensively applied tools for studying the chemical and physical properties of interfaces. These methods are intrinsically insensitive to isotropic media, and they thus overcome the main difficulty of optical studies of interfaces, namely, the fact that the linear response from the relatively small number of molecules located in the interfacial region is completely hidden by the signal from the overwhelming number of bulk molecules.

The information obtained in these experiments may have a significant value for various fields of chemistry and biochemistry,[6,7] because interfaces constitute the local environment of numerous chemical reactions and physical phenomena, including common and important processes for everyday life, such as the corrosion of metal surfaces or the formation of foams and emulsions. On the other hand, water interfaces play a key role in biological processes taking place at cell membranes, including the transport of medicines and the infection of cells by viruses. In this case, knowledge of the physical and chemical properties of the interface is essential for the design of more effective drugs.

In most cases, the SSHG or SSFG experiments do not deliver straightforward information about interfaces, and the interpretation of the results is usually difficult and sometimes ambiguous. This especially applies to SSHG, which generally provides limited spectral information, although it is a convenient and relatively simple tool for studying the orientation,[8−13] the

concentration,[14−16] and the dynamics of molecules at interfaces.[17−25]

A powerful approach to investigate physical and chemical properties of interfaces is the use of a "dynamic probe", namely, a molecule with an excited-state dynamics (for instance, its S_1 lifetime) that depends on some properties of the environment. Once the dynamics of this molecule and its dependence upon a given environment property is well-characterized by bulk spectroscopy, information on this property at the interface can then be deduced from time-resolved SSHG (TRSSHG) experiments. A good example of this approach is the measurement of the S_1 state lifetime of malachite green to characterize the microscopic friction at air/liquid and liquid/liquid interfaces.[8,26] Because the deactivation pathways of the excited state of this dye were well-understood and the dependence of its S_1 state lifetime on solvent viscosity was established, it was possible to determine the friction exerted on this molecule at various interfaces by TRSSHG. In this approach, two aspects are simultaneously investigated: (1) the properties of the interface and (2) how these properties affect the behavior of solute molecules located at the interface. A proper understanding of the interfacial process requires both issues to be addressed.

We report here on the application of the xanthene dye eosin B (EB; Figure 1) as a dynamic probe for studying the ability of a solute molecule to form hydrogen bonds with interfacial water. We have recently shown that the ultrashort S_1 state lifetime of

Figure 1. EB in its double anion form.

Figure 2. Geometry of the TRSSHG experiment.
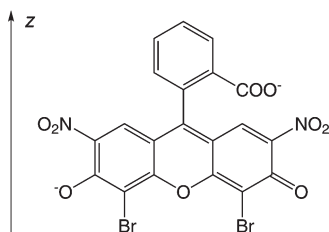
EB in protic solvents, untypical for xanthene dyes, is a result of hydrogen-bond-assisted non-radiative deactivation.[27] Consequently, the excited-state lifetime of this dye is directly related to its hydrogen-bonding properties with surrounding solvent molecules.

The excited-state deactivation mechanism of EB makes this molecule different from two other xanthene dyes, namely, rose Bengal and fluorescein,[28,29] which have also been proposed as hydrogen-bond probes. Hydrogen bonding of these two dyes with the solvent molecules results in a stabilization of the electronic states, whose magnitude depends upon the nature of the excited state. This leads to a change of the energy gap between these states, modifying the fluorescence lifetime of rose Bengal and the absorption spectrum of fluorescein. In EB, on the other hand, the absorption spectrum remains unchanged, regardless of the solvent, and, additionally, the triplet state is not populated, making this dye most convenient for TRSSHG studies.[27]

Using TRSSHG, we have monitored the decay of optically excited EB molecules at dodecane/water and decanol/water interfaces and interpreted the results in terms of the ability of interfacial water to form hydrogen bonds with EB. However, we have first studied the influence of interfacial aggregation of EB on its excited-state dynamics, to separate this effect from that of hydrogen bonding with water. Our results show that the excited-state lifetime of EB at aqueous interfaces is orders of magnitude longer than in bulk water, indicating that either the capacity of interfacial water to make hydrogen bonds with adsorbed dye molecules is strongly reduced or these bonds do not enhance the non-radiative deactivation of the excited dye molecules.

EXPERIMENTAL SECTION

EB (disodium salt, Sigma-Aldrich) was used without further purification. Dodecane and 1-decanol were used as received from Acros Organics. Water was deionized, and the pH of the aqueous solutions was kept around 9—10 by the addition of NaOH. The samples were prepared about 1 h before measurements, except for the experiments where sample aging was investigated.

The TRSSHG measurements were carried out using the geometry shown in Figure 2. The samples were contained in a 40 × 40 × 40 mm³ square glass cell and kept at room temperature (20 °C). The cell was large enough to reduce the effect of the meniscus and ensure that the surface was sufficiently flat at the center. The probe pulses, delivered directly from a Ti:Sapphire amplifier (Spitfire, Spectra Physics), were centered at 800 nm and had an energy on the sample of 10—100 nJ, duration of approximately 120 fs, and linear polarization. The direction of the polarization was controlled with a half-wave plate mounted on a motorized computer-controlled rotation stage. The angle of incidence of the probe pulses at the interface was close to the critical angle for total internal reflection. The beam was focused with a 500 mm focal length
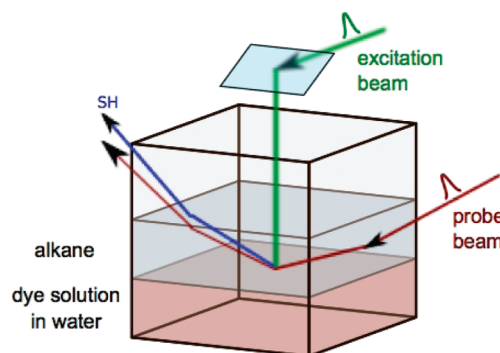
lens and passed through an absorbing filter located before the sample to eliminate second harmonic (SH) light generated at the surface of the metallic mirrors. The SH light generated at the interface was collected with a 100 mm focal length lens and passed through a plastic film polarizer on a rotating mount, which allowed selection of only one, either s- or p-polarized, component. The SH light was then filtered from the accompanying scattered fundamental light with a BG23 color filter and focused onto the entrance slit of a monochromator (0.25 m Cornerstone, Oriel) equipped with a multi-pixel photon counter avalanche photodiode detector (Hamamatsu S-10362-11-050U). The output signal was conditioned in a home-built amplifier, processed with a gated boxcar integrator and averager module (SR250, Stanford Research Systems), and finally digitized and recorded on a computer.

The 515 nm centered pump pulses were generated by a commercial non-collinear optical parametric amplifier (NOPA, Clark-MXR). The beam hitting the interface vertically from above was focused on the surface by two lenses, one spherical and one cylindrical, to match the shape of the elongated spot created on the surface by the probe beam. The energy of the pump pulses on the sample was between 1 and 2 μJ, and their polarization was circular, except for the experiment where the reorientational effects were studied and where polarization was linear.

The intensity of the SH signal was recorded as either a function of the temporal delay between the pump and probe pulses for given sets of polarization [for example, s-polarization of the probe beam (s-probe) and p-polarization of the SH light (p-SH)] or a function of the polarization angle of the probe beam at a fixed time delay and SH polarization [further referred to as polarization-dependent SSHG (PDSSHG)]. The time profiles of the TRSSHG signal were transformed by first taking the square root of the SH intensity and subsequent normalization, so that the intensity was 0 at negative time delays and 1 at the maximum time delay. The resulting profiles reflect the population dynamics of a given species at the interface, and normalization allows easy comparison between different profiles.

RESULTS AND DISCUSSION

Concentration Dependence of the SSHG Signal. Figure 3 shows PDSSHG traces measured with various bulk concentrations of EB at the dodecane/water interface. For these measurements, either the s- or p-polarization components of the SH signal were detected and the circularly polarized pump beam was either blocked or open. In the latter case, the time delay between the excitation and probe pulses was set to about 1 ps. It can be clearly seen that the shape of the PDSSHG signal strongly depends upon the dye concentration; at high concentrations, the maximum intensity of the p-SH signal is reached with the s-probe (Figure 3A), whereas at low concentrations, it is obtained
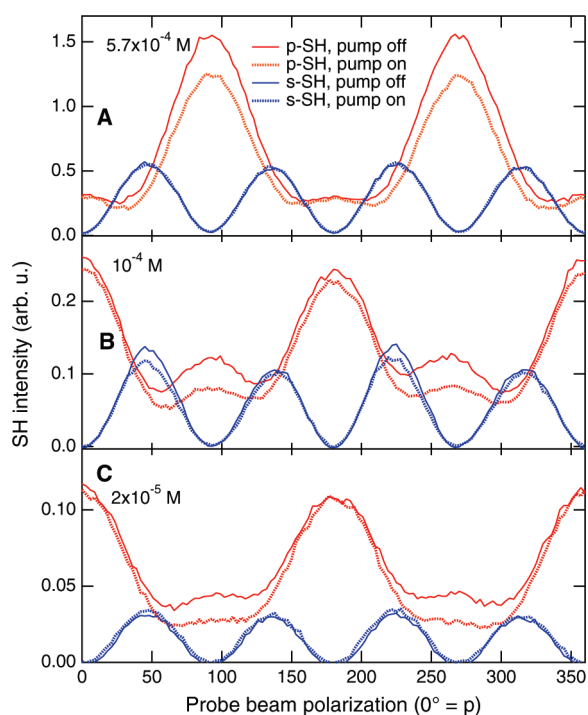
Figure 3. Dependence of the second harmonic intensity on the polarization of the probe beam measured with EB at the dodecane/water interface, without and with the pump beam at a small positive time delay, at different bulk EB concentrations (A, 5.7×10^{-4} M; B, 10^{-4} M; and C, 2×10^{-5} M).

with the p-probe (Figure 3C). At intermediate concentrations, two maxima can be seen (Figure 3B), and the dependence of the SH intensity on the polarization angle gradually changes its character with an increasing concentration. This indicates that the relative magnitude of the three non-vanishing elements ($\chi^{(2)}_{XXZ}$, $\chi^{(2)}_{ZXX}$, and $\chi^{(2)}_{ZZZ}$) of the effective second-order nonlinear susceptibility tensor, $\boldsymbol{\chi}(2)$, depends upon the EB concentration, because the SH intensity is given by[30,31]

$$I_p = B|(a_2\chi^{(2)}_{XXZ} + a_3\chi^{(2)}_{ZXX} + a_4\chi^{(2)}_{ZZZ})\cos^2\gamma$$

$$+ a_5\chi^{(2)}_{ZXX}\sin^2\gamma|^2 I^2(\omega) \qquad (1)$$

$$I_s = B|a_1\chi^{(2)}_{XXZ}\sin^2 2\gamma|^2 I^2(\omega) \qquad (2)$$

where I_p and I_s are the intensities of the p- and s-SH signal components, respectively, B and a_i are coefficients dependent on the angle of incidence and properties of the media constituting the interface, $I(\omega)$ is the incident light intensity, and γ is the angle between the direction of the probe beam polarization and the plane of incidence, so that $\gamma = 0$ for p-probe.

The above-described effect can be attributed to the formation of EB aggregates at the interface. Xanthene dyes are generally prone to aggregation,[32] and it has been shown that organic molecules at air/water or alkane/water interfaces tend to strongly aggregate, with the probability increasing with the bulk concentration of the dye.[24,26,33,34] The concentration dependence of the PDSSHG traces indicates that either the interfacial orientation of EB changes upon aggregation or the shape of the

hyperpolarizability tensor, $\boldsymbol{\beta}$, of the aggregate and the monomer differs substantially. At a given concentration, both forms contribute to the SH signal and the relative contribution of aggregates increases with the dye concentration, thus changing the effective nonlinear susceptibility tensor. A displacement of the equilibrium between the various oxidation states of EB because of pH changes could also be proposed, because this dye can exist in four different forms in aqueous solutions: double anion (Figure 1), single anion, neutral, and colorless lactone forms.[9] However, it has been shown that the pK_a of the first and second dissociation steps, which, in bulk solution, amount to 2.2 and 3.7, respectively, change to 4.0 and 4.2 at the air/water interface.[9] At the same time, it has been shown that the surface concentration of EB is low enough to keep the excess surface charge negligible. Therefore, no double layer of protons is formed at the interface to compensate for the excess negative charge, and the surface pH is equal to the bulk pH. This means that, at a bulk pH above 6, practically only one form, the double anion, is present at the interface. To ensure that this conclusion can also be drawn for the alkane/water interfaces, we checked that the PDSSHG traces had the same shape at pH values ranging from 6 to 9. Because all of the data were recorded at a pH of ~8, the hypothesis that the changes of the PDSSHG curves with the EB concentration result from a variation of the oxidation state can be ruled out.

The results of the PDSSHG measurements with various dye concentrations are consistent with previous experiments carried out at the air/water interface with $[EB] = 3 \times 10^{-5}$ M, where the intensity of the p-SH signal with s-probe was very small at pH > 6 and increased significantly at lower pH.[9] This observation was interpreted as a negligible contribution of the doubly anionic form of EB to the SSHG resonance enhancement. Nevertheless, this conclusion seems to be incorrect, because in the experiments described here, the SH signal is clearly enhanced by EB in its double anion form. Our PDSSHG measurements indicate that it is rather the orientation of EB at the interface that makes the p-SH signal with s-probe very weak at low bulk concentrations.

Figure 3 also reveals that optical excitation leads to a decrease of the p-SH intensity, with this change being the largest with s-probe and being almost absent with p-probe. On the other hand, the s-SH intensity is practically unaffected by optical excitation, independently of the polarization of the probe beam. This implies that the $\chi^{(2)}_{XXZ}$ element of the effective second-order susceptibility tensor of the system does not change upon excitation of EB, whereas $\chi^{(2)}_{ZXX}$ and $\chi^{(2)}_{ZZZ}$ change in such a way that $\Delta[a_3\chi^{(2)}_{ZXX} + a_4\chi^{(2)}_{ZZZ}] \approx 0$ (eq 1). Such a behavior of the $\chi^{(2)}_{ijk}$ tensor elements upon optical excitation has previously been observed with EB at the air/water interface[18] and was interpreted in terms of purely rotational dynamics of the molecules in the saturation regime, where population dynamics cannot be seen. In the present case, however, the experimental conditions are different and the change of the SH intensity because of optical excitation cannot be attributed to orientational effects only. First, the wavelengths of the fundamental and SH beams are relatively remote from any electronic resonances, whereas in the experiments described in ref 18, the probe beam was resonant with the $S_1 \leftarrow S_0$ transition. Second, the energies of both pump and probe pulses used here are orders of magnitude lower, preventing saturation of the electronic transitions. This difference is clearly visible in the TRSSHG data; the time profiles of the SH intensity presented in ref 18 are independent of the EB concentration,
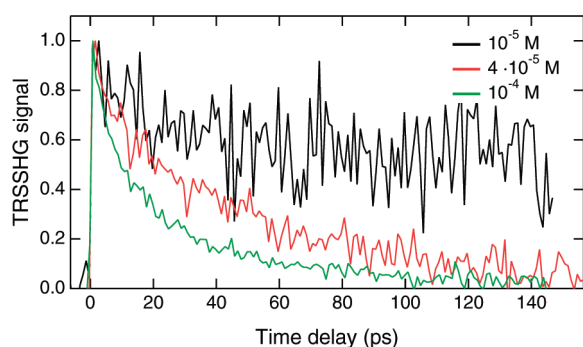
Figure 4. TRSSHG profiles (p-SH and s-probe) measured with various EB concentrations at the dodecane/water interface.

whereas a strong acceleration of the dynamics with an increasing concentration is observed here. This is illustrated in Figure 4, which depicts p-polarized TRSSHG profiles measured with s-probe and with circularly polarized pump pulses.

This concentration dependence again points to a significant role of aggregates at the interface. At the same time, it indicates that the decay of the TRSSHG signal should be mainly attributed to population relaxation and not to orientational relaxation, even though it has been shown that the latter could, in some cases, contribute to more than 80% of the decay.[19] Nevertheless, if orientational relaxation was responsible for the observed TRSSHG decays, the dynamics would slow down at higher dye concentrations, because the reorientational motion of aggregates should be slower as a result of its larger hydrodynamic volume compared to that of the monomers. This is obviously not the case here, and the observed dependence of the TRSSHG decay time on the dye concentration can be well-accounted for in terms of electronic relaxation of aggregates and monomers, because excited xanthene aggregates have been shown to undergo very efficient non-radiative deactivation.[35,36] Aggregates may also reduce the excited-state lifetime of monomers through excitation energy-transfer quenching. However, it is difficult to determine whether the latter process is really operative at the interface. Because both monomers and aggregates probably contribute to the resonant enhancement of the SH intensity, the overall TRSSHG signal decay should be faster at higher concentrations of aggregates, even if the latter do not quench the excited monomers.

Effect of Sample Aging. There is still an additional effect that can be associated with interfacial aggregation; PDSSHG and TRSSHG curves recorded at the dodecane/water interface change slowly but significantly with time. For instance, the PDSSHG traces measured with a fresh 2×10^{-5} M EB sample have only maxima with p-probe. Several hours after sample preparation, small local maxima appear with s-probe, and 1 day later, these maxima predominate (Figure 5A). This variation of the PDSSHG traces is accompanied by changes in the TRSSHG dynamics; the decays become faster with the time elapsed after sample preparation (Figure 5B). A similar effect is also observed at higher EB concentrations. At 10^{-4} M, the global maxima of the p-polarized PDSSHG curves (Figure 3B) disappear entirely after 24 h and the PDSSHG traces recorded with a 1-day-old sample look like those measured with a fresh and more concentrated EB sample (Figure 3A). In this case, however, the shortening of the decay time is much less pronounced but can still be seen. In general, sample aging has the same effect on the measured SSHG
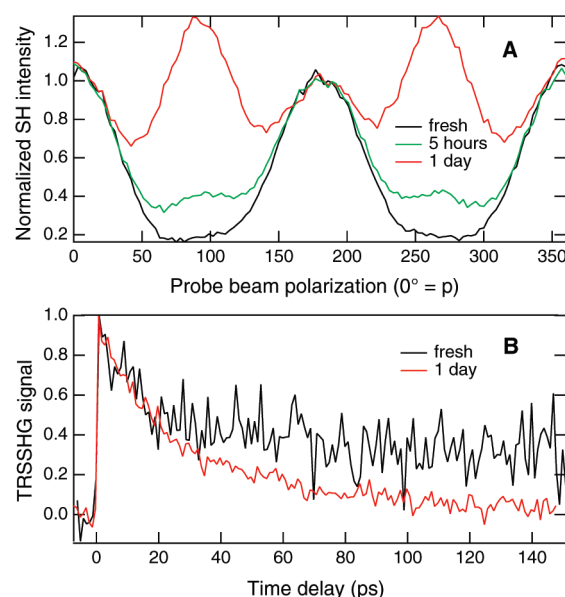

Figure 5. (A) Dependence of the p-SH intensity on the polarization of the probe beam measured at the dodecane/water interface with fresh, 5 h, and 1-day-old samples ([EB] = 2×10^{-5} M) and (B) time profiles of the TRSSHG intensity measured with fresh and 1-day-old samples.

data as an increase of the EB concentration. This leads us to conclude that, in both cases, the changes stem from an increasing concentration of aggregates at the interface, that aggregation at low dye concentration is very slow, and thus, that the equilibrium between aggregates and monomers needs several hours to be fully established at the interface.

Because of this strong tendency of EB to aggregate at the dodecane/water interface, only TRSSHG profiles recorded with fresh samples at low concentrations can be compared to the data measured in bulk solutions, where monomers are almost exclusively present. These conditions are very unfavorable for the interfacial measurements, because the SH signal has to be detected with s-probe, i.e., at a minimum of the PDSSHG curves. Consequently, the intensity of the detected signal is very low (Figure 3C), and the noise of the TRSSHG profiles is high (Figure 4).

EB at the Decanol/Water Interface. In addition to the studies of EB at the dodecane/water interface, measurements at the decanol/water interface have also been carried out. Decanol is weakly miscible with water, and the solubility of EB in this solvent is rather low. This, together with the high viscosity of decanol, slows down the diffusion of EB from the aqueous to decanol phases and makes such experiments possible. The replacement of an alkane by a long-chain alcohol has a strong impact on the observed SSHG signals. First, the SH intensity is much lower than with dodecane/water, so that measurements were practically impossible at EB concentrations below 5×10^{-4} M. Despite this, the PDSSHG traces at higher EB concentrations with decanol look similar to those with dodecane at low concentrations (Figure 6A).

Second, in contrast to the dodecane/water interface, the decanol/water samples do not exhibit any influence of aging (Figure 6B). These differences indicate that EB does not aggregate easily at the decanol/water interface. This most likely stems from the higher water solubility of decanol compared to dodecane that should result in a more diffuse nature of the decanol/water interface compared to the dodecane/water interface. With decanol, the EB molecules diffusing from the aqueous
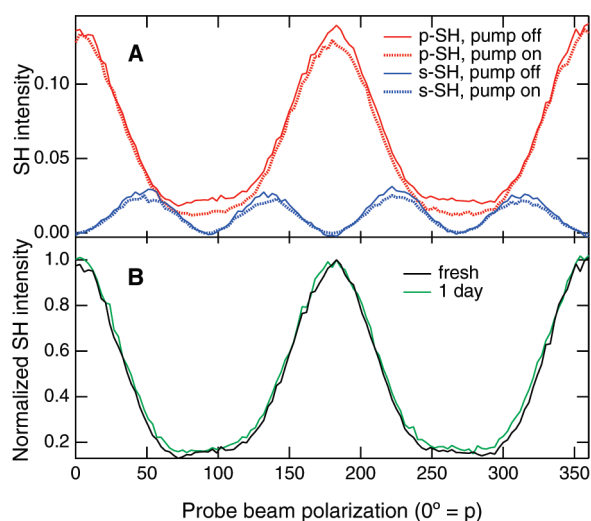
Figure 6. (A) Dependence of the second harmonic intensity on the polarization of the probe beam measured with EB $(5.7 \times 10^{-4}$ M) at the decanol/water interface, with and without the pump beam at a small positive delay, and (B) dependence of the p-SH intensity on the polarization of the probe beam at the decanol/water interface recorded with fresh and 1-day-old samples.
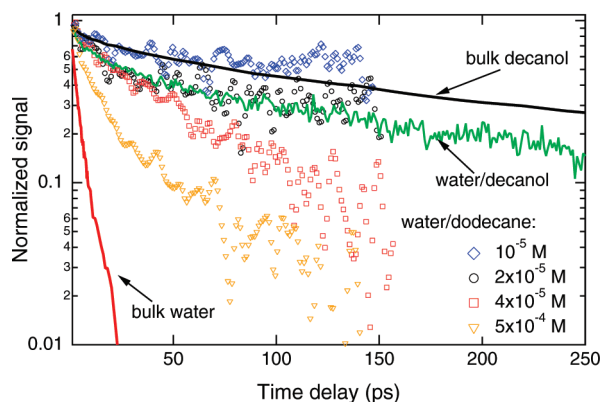

Figure 7. Comparison of time profiles recorded by transient absorption with bulk water and decanol solutions of EB (red and black solid lines)[27] and TRSSHG at the dodecane/water interface with various EB concentrations (markers) and at the decanol/water interface (green line; [EB] = 5.7×10^{-4} M).

phase toward the interface do not encounter the alkane barrier, where they are insoluble, but rather a region where water and decanol coexist. Most likely, EB is better solvated in this diffuse interfacial layer than at the "sharp" dodecane interface, and consequently, aggregation is much less favorable.

Interfacial Hydrogen Bonding. Figure 7 depicts a comparison of TRSSHG profiles measured at both dodecane/water and decanol/water interfaces with transient absorption profiles recorded in bulk water and decanol at a wavelength reflecting the ground-state recovery of EB.[27] It is clear that, even with the significant contribution of aggregates at high EB concentrations, the decays measured at interfaces are all much slower than in bulk water.

The ultrashort excited-state deactivation of EB in water has been explained in terms of hydrogen-bond-assisted non-radiative

deactivation.[27] Because of the charge-transfer character of the $S_1 \leftarrow S_0$ transition, the electron density at the nitro groups increases significantly upon excitation, strengthening the coupling with the surrounding protic solvent molecules. As a consequence, the S_1 lifetime of EB decreases significantly with an increasing hydrogen-bonding ability of the solvent.[27] Therefore, the slow excited-state dynamics measured by TRSSHG leads us to conclude that EB is much less hydrogen-bonded with interfacial water than with bulk water. This interpretation agrees well with a previous study of EB at air/water interfaces,[18] where the reorientational dynamics of EB was compared to that of rhodamine 6G (R6G). Whereas the rotational time of EB at the air/water interface was found to be much faster than in bulk water, the opposite trend was reported for R6G.[37] This effect has been explained by the authors of ref 18 by a strengthening of the hydrogen-bonding network between interfacial water molecules. Because of this, hydrogen bonding of a solute molecule to interfacial water is much less efficient. As a consequence, EB can rotate more easily at the interface than in bulk water, where it is strongly hydrogen-bonded. On the other hand, the larger rotational time of R6G at the interface was explained by an absence of a hydrogen bond with bulk water and by the more rigid, hydrogen-bonded, interfacial water structure.[18]

Hydration of small nonpolar organic molecules[38] and macro-molecules, such as proteins,[39−42] is accompanied by a strengthening of water−water hydrogen bonds as a consequence of the weak water solubility of these solutes. Early vibrational SSFG studies of nonpolar liquid/water interfaces seemed to indicate an absence of hydrogen-bond strengthening at macroscopic interfaces, such as CCl_4/water or hexane/water, because the interfacial infrared spectra were lacking the features of strongly hydrogen-bonded water.[43,44] Later, this conclusion has been contradicted by molecular-dynamics simulations that revealed the existence of a large population of strongly hydrogen-bonded water molecules at the interface, in addition to monomer-like water molecules. Their orientation, however, parallel to the interfacial plane, makes these bonds undetectable by vibrational SSFG.[45,46]

The ability of interfacial water to act as a strong hydrogen-bond donor has been confirmed by SSHG studies of N-methyl-p-methoxyaniline (NMMA) at the CCl_4/water interface.[47] The SSHG spectra of NMMA, whose electronic absorption spectrum is sensitive to the hydrogen-bonding properties of the environment, were typical for strong hydrogen bonds with water.

The results of our TRSSHG studies with EB at alkane/water interfaces are rather surprising in view of the above experiments, revealing that a significant fraction of interfacial water molecules can be a donor of strong hydrogen bonds. At least two hypotheses can be proposed: (1) Hydrogen bonding of EB with interfacial water could be inhibited by the location of the nitro-substituents, which are directly involved in the non-radiative deactivation of EB, in the nonpolar phase, even though this seems improbable considering the polar and anionic nature of the xanthene moiety. Still, if the hydrogen-bond-accepting strength of the carboxylic group prevails over the affinity of the xanthene moiety for the polar phase, the molecules can be oriented in such a way that the nitro groups have limited contact with interfacial water. (2) EB might still be hydrogen-bonded with the interfacial water molecules, but the hydrogen-bond-assisted deactivation pathway might be inoperative at the interface. Although this non-radiative process has been reported with many different chromophores in protic solvents,[48−53] its exact mechanism is still not

totally understood. This process could be viewed as an excited-state intermolecular proton transfer with the solvent molecules, followed by back proton transfer to the ground state. Possibly the interfacial environment is such that this process is no longer efficient.

Unfortunately, our results do not provide any evidence in favor or against one of these hypotheses. Moreover, our PDSSHG data do not provide easily accessible information on the orientation of EB molecules at the interfaces. This is due to the probe wavelength that does not coincide with an electronic transition of this dye. Because of this, no assumption on the components of the hyperpolarizability tensor can be performed. Previous measurements with EB at the air/water interface with a probe wavelength close to the maximum of the $S_1 \leftarrow S_0$ absorption band revealed that the angle between the z axis of EB (Figure 1) and the surface normal is about $25-30°$.[18] Further studies are needed to determine the orientation of EB molecules at liquid/liquid interfaces. This could give insight into the mechanism behind the long excited-state lifetime of this dye at interfaces.

The TRSSHG profiles, $A(t)$, shown in Figure 7, can be analyzed with a bi-exponential function convolved with the instrument response function, $f(t)$

$$A(t) = \left[A_0 + A_1 \exp\left(-\frac{t}{\tau_1}\right) + A_2 \exp\left(-\frac{t}{\tau_2}\right) \right] \otimes f(t) \tag{3}$$

where τ_1 and τ_2 are associated with the initial decay and the constant amplitude, A_0, is related to the long-lived excited-state population. An unequivocal assignment of τ_1 and τ_2 is not possible, because the initial decay can result from various processes: (1) fast radiationless deactivation of excited EB aggregates, (2) excitation energy hopping, and/or (3) hydrogen-bond-assisted deactivation of a small population of EB molecules able to bind with water. The assignment of τ_1 and τ_2 is even more complicated because three decay constants are required to describe the excited-state dynamics of EB in bulk water solution. Therefore, only the amplitude of the long-lived component, A_0, can be interpreted, but its associated time constant cannot be determined because of the limited temporal window of the experiment.

The magnitude of A_0 (with $A_0 + A_1 + A_2 = 1$) can be used to estimate the minimum fraction of EB molecules belonging to the long-lived population. Assuming that the initial decay is entirely due to hydrogen-bond-assisted deactivation, A_0 is equal to the long-lived fraction of the total number of adsorbed EB molecules. This fraction is even higher if processes 1 and/or 2 also contribute to the initial decay.

In fact, it can be shown that the initial decay partially results from processes 1 and 2. First, the plot of A_0 versus [EB] (Figure 8A) exhibits a steep decrease at low concentrations. This means that the limit at which only monomers are present at the interface is not reached at the lowest concentration used, because otherwise A_0 would be independent of the bulk EB concentration for small [EB]. Therefore, even at the lowest EB concentration used in the experiments, $[EB] = 10^{-5}$ M, the aggregates are still present at the interface and contribute to the fast decay.

Second, the TRSSHG profiles measured with linearly polarized pump pulses are different, with light polarized parallel and perpendicular to the plane of incidence of the probe pulses, as
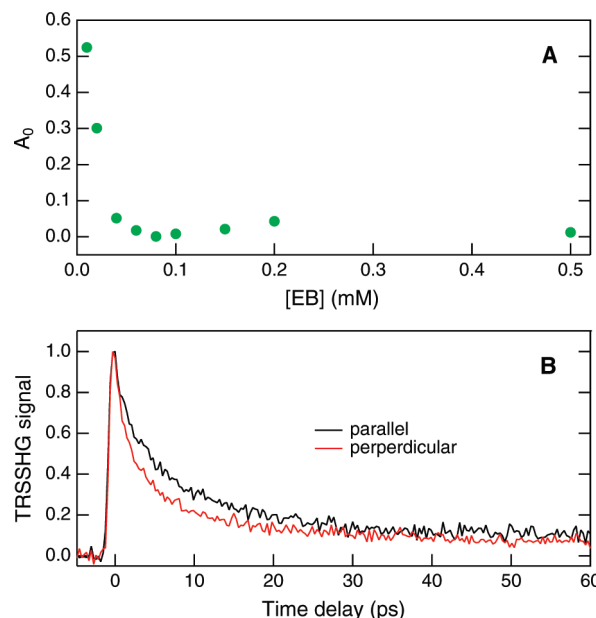

Figure 8. (A) EB concentration dependence of the long-lived component of the TRSSHG profiles measured at the dodecane/water interface and (B) TRSSHG profiles measured with EB at the dodecane/water interface with pump pulses linearly polarized parallel and perpendicular to the plane of incidence of the probe pulses.

illustrated in Figure 8B with $[EB] = 10^{-4}$ M. This means that depolarization phenomena could to a certain extent contribute to the measured signal decays.[19] However, this polarization dependence takes place on too short a time scale ($\sim 10-20$ ps) to be attributed to the reorientational motion of a molecule of the size of EB. For example, the reorientation time of a molecule of similar size in a polar but nonprotic solvent of the same viscosity as water is on the order of 140 ps.[54] The interfacial EB concentration is not known, but considering that aggregation takes place, it can be expected to be substantially larger than the bulk concentration. Therefore, the pump polarization dependence of the TRSSHG decay most likely originates from excitation energy hopping between interfacial EB molecules.

In summary, the fraction of EB molecules adsorbed at the dodecane/water interface that are not affected by the mechanism of hydrogen-bond-assisted excited-state deactivation substantially exceeds a lower limit of 50% at $[EB] = 10^{-5}$ M (Figure 8A).

The decay of the TRSSHG signal at the decanol/water interface is faster than in bulk decanol and resembles that recorded at the dodecane/water interface with $[EB] = 2 \times 10^{-5}$ M. It is, however, difficult to determine whether this is due to a higher contribution of aggregates at the larger EB concentration used in this case (5.7×10^{-4} M) or rather a result from an intrinsic difference between the nonpolar liquid/water and polar liquid/water interfaces. Interfacial decanol molecules can be expected to be oriented with their hydroxyl groups toward the aqueous phase and to make hydrogen bonds with water. Further studies of interfaces between long-chain alcohols and water are needed before more definitive conclusions can be drawn.

■ CONCLUDING REMARKS

This study shows that, because its S_1 state undergoes hydrogen-bond-assisted non-radiative deactivation, EB can be used as a

dynamic probe for investigating hydrogen bonding at alkane/water and long-chain alcohol/water interfaces by TRSSHG. However, its application is complicated by the formation of interfacial aggregates that also leads to a shortening of the TRSSHG decay. Nevertheless, this effect can be minimized when working at low concentrations and, below 2×10^{-5} M, the TRSSHG signal is dominated by EB monomers. In such conditions, we were able to see that the TRSSHG signal at the dodecane/water interface is dominated by a slow, >1 ns, decaying component, whereas the S_1 lifetime of EB in bulk water is on the order of a few picoseconds. This huge difference points to the existence of a large population of EB molecules (exceeding 50% of the total surface population at $[EB] = 10^{-5}$ M), which are not hydrogen-bonded to the solvent or, at least, do not undergo hydrogen-bond-assisted non-radiative deactivation. This difference between EB and NMMA, which was found to be strongly hydrogen-bonded to interfacial water molecules, may arise from a specific orientation of EB molecules at the interface, which prevents contact between the hydrogen-bond-accepting nitro groups and water, or from the mechanism of the hydrogen-bond-assisted deactivation itself that is no longer operative at the interface. The discrepancy between the experiments with EB and NMMA shows how the properties of a particular probe molecule may affect the results of interfacial measurements. Thus, it is important to carry out such experiments with various techniques and probe molecules to be able to draw general conclusions on the nature of an interface.

The above findings may also be summarized in a different way; the S_1 state of EB that is nonfluorescent in aqueous solutions becomes long-lived and, thus, fluorescent once EB is adsorbed at a liquid/water interface. This opens a possibility to study interfaces by fluorescence techniques if the ratio of adsorption to bulk molecules is sufficiently large to make the bulk background fluorescence negligible. Because of the ultra-short excited-state lifetime of EB in water, this condition should be possible to satisfy in systems such as emulsions, protein solutions, nanoparticles dispersed in water, or colonies of living cells, provided that the results from the alkane/water interfaces studied here are general and transferable to other systems of similar nature. One could think of using EB to measure the total surface of nanoparticles dispersed in water by detecting the fluorescence of the sample and relating its intensity to the total area of their interface with water. Preliminary experiments have shown that the fluorescence intensity of EB in aqueous solution increases upon adsorption on micelles formed after the addition of a surfactant to the solution. Further studies are required to test the applicability of EB and other molecules deactivated in a hydrogen-bond-assisted process as fluorescent probes of interfacial properties, but if they appear to be positive, this may become a powerful technique applicable to various fields of surface chemistry and biology.

■ AUTHOR INFORMATION

Corresponding Author
*E-mail: eric.vauthey@unige.ch.

Present Addresses
[†]Institute of Experimental Physics, Faculty of Physics, University of Warsaw, Ulica Hoża 69, 00-681 Warsaw, Poland.

■ REFERENCES

(1) Eisenthal, K. B. *Chem. Rev.* **1996**, *96*, 1343.
(2) Brevet, P.-F. *Surface Second Harmonic Generation*; Presses Polytechniques et Universitaires Romandes: Lausanne, Switzerland, 1997.
(3) Benjamin, I. *Chem. Rev.* **2006**, *106*, 1212.
(4) Richmond, G. L. *Chem. Rev.* **2002**, *102*, 2693.
(5) Sekiguchi, K.; Yamaguchi, S.; Tahara, T. *J. Chem. Phys.* **2008**, *128*, 114715.
(6) *Liquid Interfaces in Chemical, Biological, and Pharmaceutical Applications*; Volkov, A. G., Ed.; Marcel Dekker: New York, 2001.
(7) *Interfacial Nanochemistry*; Watarai, H., Teramae, N., Sawada, T., Eds.; Kluwer Academic: New York, 2005.
(8) Shi, X.; Borguet, E.; Tarnovsky, A. N.; Eisenthal, K. B. *Chem. Phys.* **1996**, *205*, 167.
(9) Tamburello-Luca, A. A.; Hebert, P.; Antoine, R.; Brevet, P. F.; Girault, H. H. *Langmuir* **1997**, *13*, 4428.
(10) Tsukanova, V.; Slyadneva, O.; Inoue, T.; Harata, A.; Ogawa, T. *Chem. Phys.* **1999**, *250*, 207.
(11) Lin, S.; Meech, S. R. *Langmuir* **2000**, *16*, 2893.
(12) Steinhurst, D. A.; Owrutsky, J. C. *J. Phys. Chem. B* **2001**, *105*, 3062.
(13) Sen, S.; Yamaguchi, S.; Tahara, T. *Angew. Chem., Int. Ed.* **2009**, *48*, 6439.
(14) Petersen, P. B.; Saykally, R. J. *Chem. Phys. Lett.* **2004**, *397*, 51.
(15) Petersen, P. B.; Saykally, R. J. *J. Phys. Chem. B* **2006**, *110*, 14060.
(16) Onorato, R. M.; Otten, D. E.; Saykally, R. J. *Proc. Natl. Acad. Sci. U.S.A.* **2009**, *106*, 15176.
(17) Meech, S. R.; Yoshihara, K. *J. Phys. Chem.* **1990**, *94*, 4913.
(18) Antoine, R.; Tamburello-Luca, A. A.; Hébert, P.; Brevet, P. F.; Girault, H. H. *Chem. Phys. Lett.* **1998**, *288*, 138.
(19) Zimdars, D.; Dadap, J. I.; Eisenthal, K. B.; Heinz, T. F. *J. Phys. Chem. B* **1999**, *103*, 3425.
(20) Benderskii, A. V.; Eisenthal, K. B. *J. Phys. Chem. B* **2000**, *104*, 11723.
(21) Shang, X.; Benderskii, A. V.; Eisenthal, K. B. *J. Phys. Chem. B* **2001**, *105*, 11578.
(22) Steinhurst, D. A.; Baronavski, A. P.; Owrutsky, J. C. *J. Phys. Chem. B* **2002**, *106*, 3160.
(23) McArthur, E. A.; Eisenthal, K. B. *J. Am. Chem. Soc.* **2006**, *128*, 1068.
(24) Punzi, A.; Martin-Gassin, G.; Grilj, J.; Vauthey, E. *J. Phys. Chem. C* **2009**, *113*, 11822.
(25) Song, J.; Kim, M. W. *J. Phys. Chem. B* **2010**, *114*, 3236.
(26) Fita, P.; Punzi, A.; Vauthey, E. *J. Phys. Chem. C* **2009**, *113*, 20705.
(27) Fita, P.; Fedoseeva, M.; Vauthey, E. *J. Phys. Chem. A* **2011**, *115*, DOI: 10.1021/jp110849x.
(28) Cramer, L. E.; Spears, K. G. *J. Am. Chem. Soc.* **1978**, *100*, 221.
(29) Klonis, N.; Clayton, A. H. A.; Voss, E. W.; Sawyer, W. H. *Photochem. Photobiol.* **1998**, *67*, 500.
(30) Brevet, P. F. *J. Chem. Soc., Faraday Trans.* **1996**, *92*, 4547.
(31) Antoine, R.; Bianchi, F.; Brevet, P. F.; Girault, H. H. *J. Chem. Soc., Faraday Trans.* **1997**, *93*, 3833.
(32) Valdes-Aguilera, O.; Neckers, D. C. *Acc. Chem. Res.* **1989**, *22*, 171.
(33) Brodard, P.; Vauthey, E. *Rev. Sci. Instrum.* **2003**, *74*, 725.
(34) Fedoseeva, M.; Fita, P.; Punzi, A.; Vauthey, E. *J. Phys. Chem. C* **2010**, *114*, 13774.
(35) Penzkofer, A.; Lu, Y. *Chem. Phys.* **1986**, *103*, 399.

(36) De, S.; Das, S.; Girisgoswami, A. *Spectrochim. Acta, Part A* **2005**, *61*, 1821.

(37) Castro, A.; Sitzmann, E. V.; Zhang, D.; Eisenthal, K. B. *J. Phys. Chem.* **1991**, *95*, 6752.

(38) Silverstein, T. P. *J. Chem. Educ.* **1998**, *75*, 116.

(39) Chothia, C.; Janin, J. *Nature* **1975**, *256*, 705.

(40) Wiggins, P. M. *Phys. A* **1997**, *238*, 113.

(41) Robinson, G. W.; Cho, C. H. *Biophys. J.* **1999**, *77*, 3311.

(42) Ball, P. *Chem. Rev.* **2007**, *108*, 74.

(43) Scatena, L. F.; Brown, M. G.; Richmond, G. L. *Science* **2001**, *292*, 908.

(44) Scatena, L. F.; Richmond, G. L. *J. Phys. Chem. B* **2001**, *105*, 11240.

(45) Moore, F. G.; Richmond, G. L. *Acc. Chem. Res.* **2008**, *41*, 739.

(46) McFearin, C. L.; Beaman, D. K.; Moore, F. G.; Richmond, G. L. *J. Phys. Chem. C* **2009**, *113*, 1171.

(47) Siler, A. R.; Brindza, M. R.; Walker, R. A. *Anal. Bioanal. Chem.* **2009**, *395*, 1063.

(48) Inoue, H.; Hida, M.; Nakashima, N.; Yoshihara, K. *J. Phys. Chem.* **1982**, *86*, 3184.

(49) Flom, S. R.; Barbara, P. F. *J. Phys. Chem.* **1985**, *89*, 4489.

(50) Yatsuhashi, T.; Inoue, H. *J. Phys. Chem. A* **1997**, *101*, 8166.

(51) Cser, A.; Nagy, K.; Biczok, L. *Chem. Phys. Lett.* **2002**, *360*, 473.

(52) Fürstenberg, A.; Vauthey, E. *Photochem. Photobiol. Sci.* **2005**, 260.

(53) Sherin, P. S.; Grilj, J.; Kopylova, L. V.; Yanshole, V. V.; Tsentalovich, Y. P.; Vauthey, E. *J. Phys. Chem. B* **2010**, *114*, 11909.

(54) Vauthey, E. *Chem. Phys. Lett.* **1993**, *216*, 530.